

Supporting Information

Efficient bandgap widening of co-evaporated MAPbI_3 perovskite

Herlina Arianita Dewi^a, Jia Li^a, Enkhtur Erdenebileg^a, Hao Wang^a, Michele De Bastiani,^b Stefaan De Wolf,^b Nripan Mathews^{ac}, Subodh Mhaisalkar^{ac*}, Annalisa Bruno^{a*}*

^a Energy Research Institute @ NTU (ERI@N), Nanyang Technological University, 637553, Singapore

^b KAUST Solar Center (KSC), Physical Sciences and Engineering Division (PSE), King Abdullah University of Science and Technology (KAUST), Thuwal, 23955-6900, Kingdom of Saudi Arabia.

^c School of Materials Science & Engineering, Nanyang Technological University, 639798, Singapore

*Corresponding author: annalisa@ntu.edu.sg, subodh@ntu.edu.sg, nripan@ntu.edu.sg

Experimental Section

Perovskite Absorber

MAPbI₃ with excess PbI₂ was deposited using the co-evaporation deposition method [2], employing PbI₂ powder (TCI) and MAI powder (Lumtec). The PbI₂ source was set at 260 °C and the MAI source was set at 100 °C with a total deposition time of 180 mins inside a vacuum chamber with a base starting chamber pressure of 8*10⁻⁶ Torr. Upon deposition, the MAPbI₃ film was subsequently annealed at 100 °C for 30 mins. QCM deposition rate was not given due to instability of the QCM reading due to MAI background pressure.

MAPb(Br_xI_{1-x})₃ was prepared using as-deposited MAPbI₃ as a template. The 750 nm MAPbI₃ is chosen since it results in the highest PCE [27]. The MABr (Greatcell) is dissolved in anhydrous isopropanol (IPA) with concentrations ranging from 5 - 15 mg/mL. The as-deposited MAPbI₃ was then subjected to MABr/IPA treatment with a different conversion time of 1 min and 5 mins respectively, followed by spin coating at 5000 rpm for 30 s to remove unreacted MABr/IPA and consequently being annealed at 100 °C for 30 mins.

Perovskite solar cell fabrication

Fluorine-doped tin oxide (FTO) glass substrates were cleaned using decon soap, water, and ethanol. Low-temperature bilayer p-SnO₂/PCBM is used as an electron transport layer, following previous procedures [2]. The Spiro-OMeTAD (70 mg/mL in chlorobenzene) (Lumtec) was prepared with addition of 28.5 μL 4-tert-butylpyridine (Sigma Aldrich) and 17.5 μL bis(trifluoromethane)sulfonamide lithium salt (Sigma Aldrich) solution (520 mg/mL in ACN). The Spiro-OMeTAD is deposited by spin-coating at 5000 rpm for 30 s. The PTAA solution is prepared by dissolving PTAA (EM Index) with concentration of 10 mg/mL inside toluene. 4 μL 4-tert-butylpyridine (Sigma Aldrich) and 6 μL bis(trifluoromethane)sulfonamide lithium salt (Sigma Aldrich) solution (170 mg/mL in ACN). The PTAA spin coating condition is at 5000 rpm for 30 s. A 100 nm gold electrode was deposited as back contact using thermal evaporation.

Textured silicon substrates

Polished wafers (Topsil) are textured in alkaline (KOH) solution to obtain randomly distributed pyramids. To accommodate the evaporated perovskite films, the size of the pyramids is controlled with different KOH concentrations, targeting pyramid sizes in the range of 5-7 μm. The wafers have been then cleaned with a standard RCA process as reported elsewhere.

Characterization

Morphological characterization was recorded using a Field Emission Scanning Electron Microscope (FESEM, JEOL JSM-7600F, 5 kV, and 10 mA). The absorbance was recorded using UV-Vis-NIR Spectrophotometer (UV3600, Shimadzu). The steady photoluminescence spectra were measured by Spectro-fluorophotometer (Shimadzu, RF-5301PC). The current density-voltage (J-V) curves were measured using Newport Oriel Sol3ATM solar simulator with a 450-Watt Xenon lamp which is calibrated using a standard silicon solar cell. The active area of 0.086 cm² was determined by a metal shadow mask. The incident photon-to-current conversion efficiency (IPCE) was measured by using a PVE300 (Bentham), with a dual xenon/quartz halogen light source in DC mode Newport Oriel. The XRD patterns of the thin films were recorded using X-ray diffraction (XRD; Bruker D8 Advance XRD). The XPS was conducted using Kratos AXIS Supra.

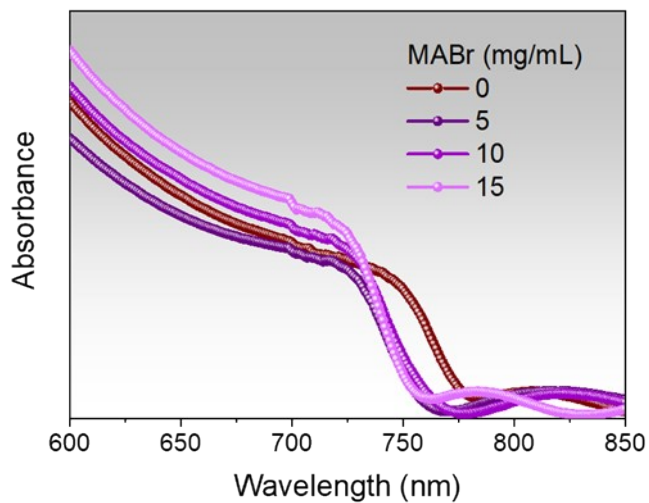


Fig. S1. The absorbance of MAPbI_3 and $\text{MAPbI}_3+\text{MABr}$ treated with various MABr concentrations

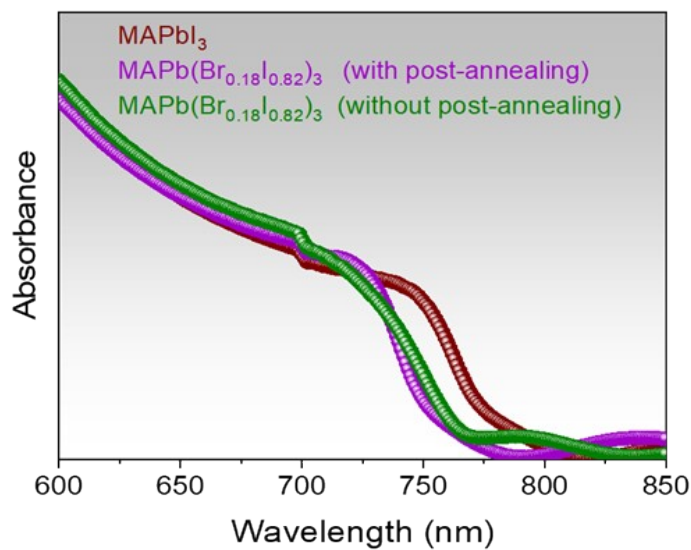


Fig S2. The absorbance of MAPbI_3 and $\text{MAPb}(\text{Br}_{0.18}\text{I}_{0.82})_3$ with (purple) and without post-annealing (green) at 100 °C for 30 mins

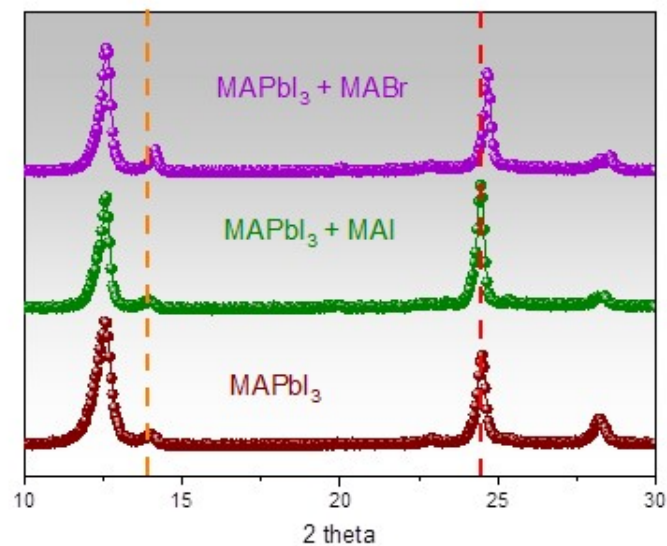


Fig. S3. XRD patterns of MAPbI_3 (brown), $\text{MAPbI}_3 + \text{MAI}$ (green), and $\text{MAPbI}_3 + \text{MABr}$ (purple) treated for 1 minute. The $<110>$ perovskite peak (orange line) and $<202>$ perovskite peak (red line) for MAPbI_3

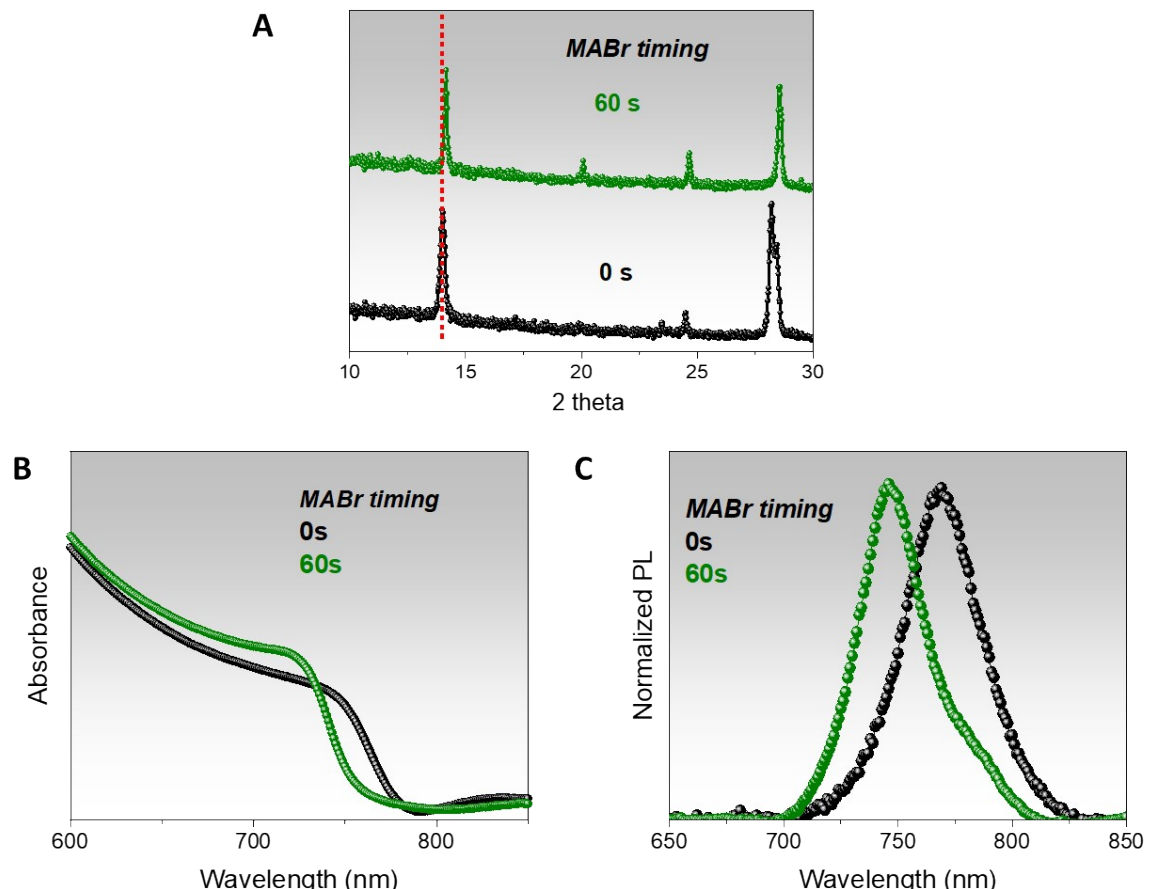


Fig. S4. MABr treatment on stoichiometric grown co-evaporated MAPbI_3 . (A) XRD patterns. The red dotted line shows the $<110>$ perovskite growth orientation. (B) Absorbance, and (C)

Normalized steady-state photoluminescence, of MAPbI_3 (black) and MAPbI_3 treated with MABr for 60 s (green).

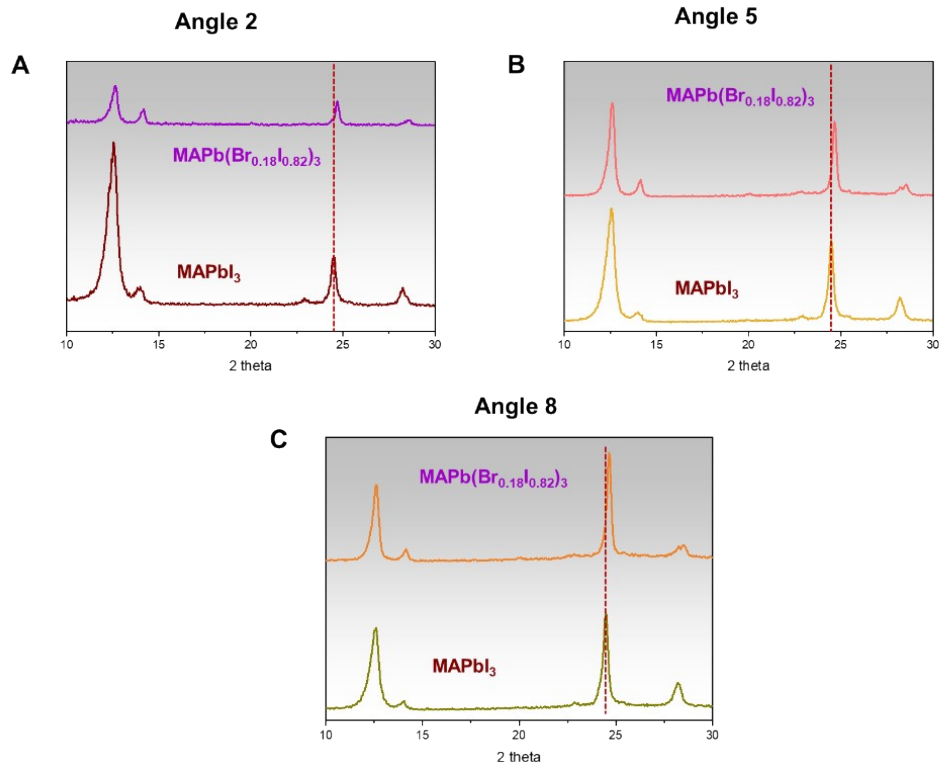


Fig. S5. The non-normalized XRD spectra were taken at (A) 2° , (B) 5° , and (C) 8° XRD angle for both MAPbI_3 and $\text{MAPb}(\text{Br}_{0.18}\text{I}_{0.82})_3$ films. The dotted lines represent $<202>$ perovskite orientation for MAPbI_3 composition.

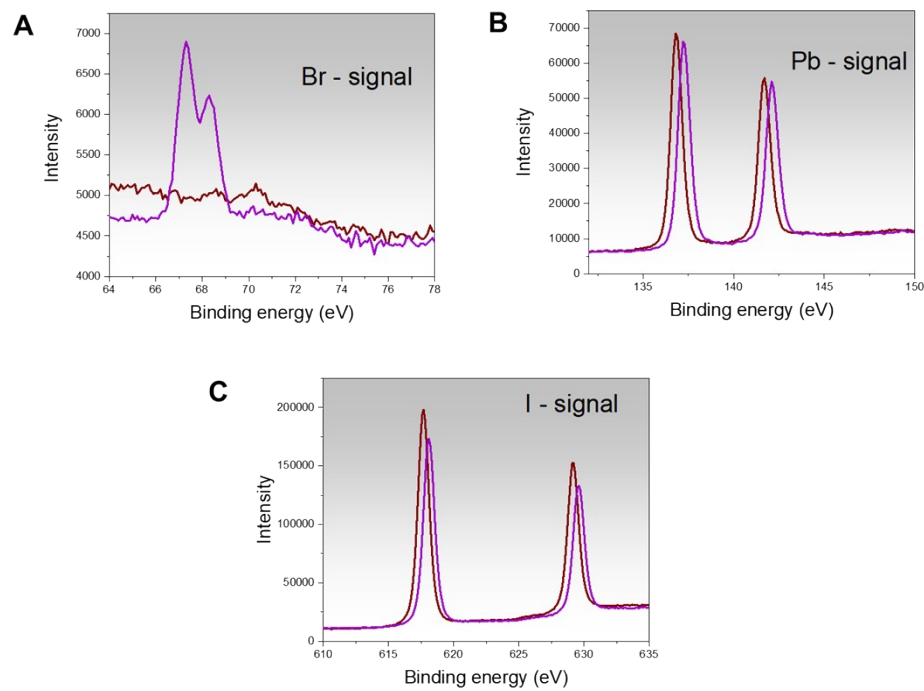


Fig. S6. XPS of MAPbI_3 (brown) and $\text{MAPb}(\text{Br}_{0.18}\text{I}_{0.82})_3$ (purple) films (A) Br, (B) Pb, and (C)

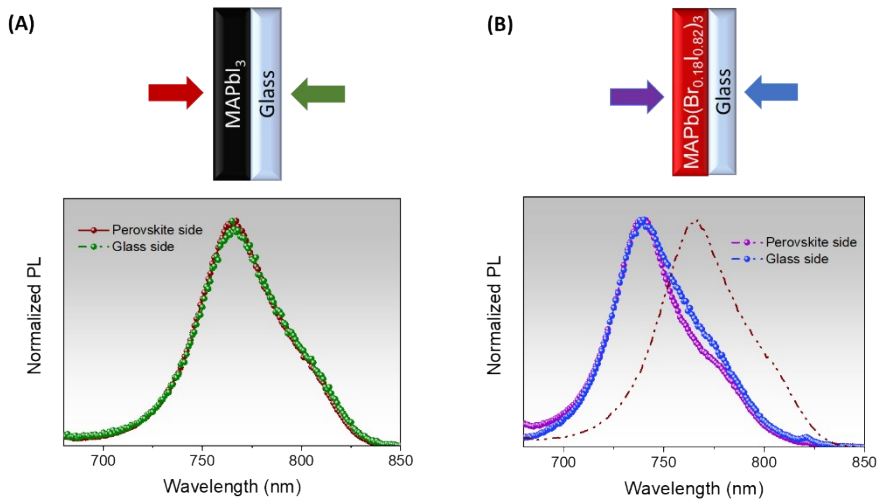


Fig. S7. Schematic of steady-state photoluminescence taken from both perovskite and glass side for (A) MAPbI_3 and (B) $\text{MAPb}(\text{Br}_{0.18}\text{I}_{0.82})_3$ films, the dotted brown line refer to steady-state photoluminescence of MAPbI_3 .

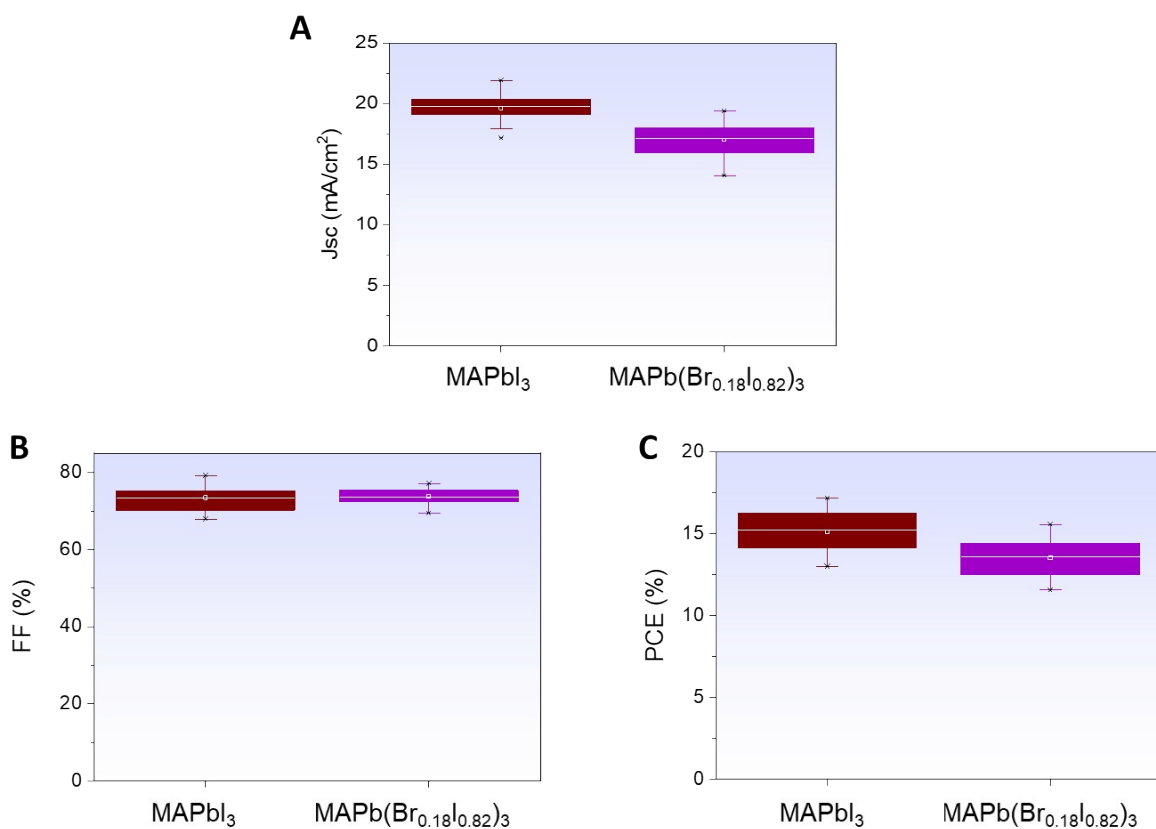


Fig. S8. Photovoltaic parameters of n-i-p PSCs based on Spiro-OMeTAD as HTM (A) J_{sc} , (B) FF, and (C) PCE for MAPbI_3 (brown) and $\text{MAPb}(\text{Br}_{0.18}\text{I}_{0.82})_3$ (purple).

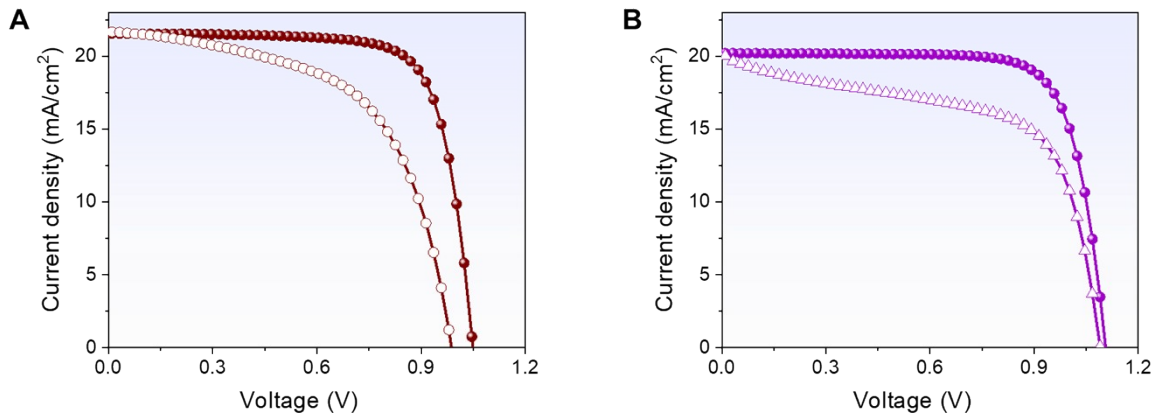


Fig. S9 J-V curves of Spiro-OMeTAD HTL based PSCs using (A) MAPbI_3 and (B) $\text{MAPb}(\text{Br}_{0.18}\text{I}_{0.82})_3$ perovskite compositions taken from reverse (solid) and forward (hollow) scan direction.

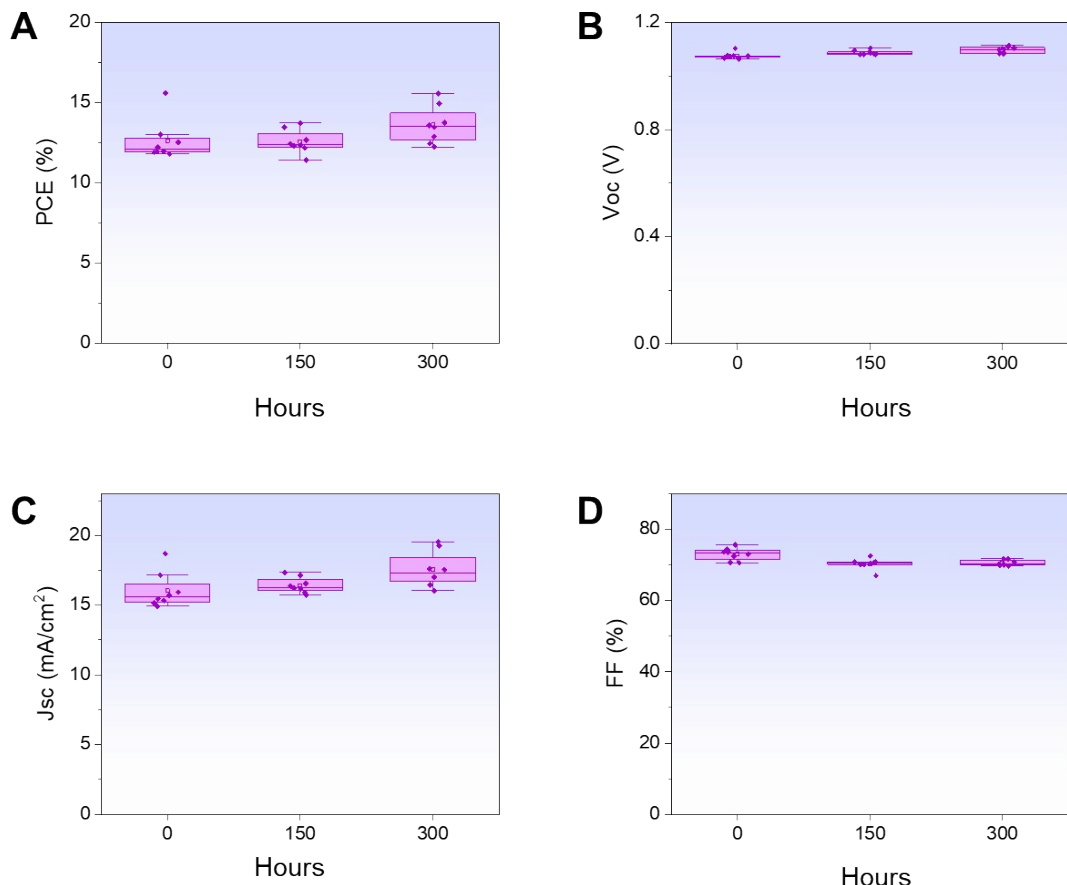


Fig. S10. Shelf stability of $\text{MAPb}(\text{Br}_{0.18}\text{I}_{0.82})_3$ PSCs with Spiro-OMeTAD as HTM. Photovoltaic parameters (A) PCE, (B) Voc, (C) J_{sc} , and (D) FF of PSCs based on

MAPb($\text{Br}_{0.18}\text{I}_{0.82}$)₃ when stored at room temperature and in a controlled environment with 30% RH for 300 hours.

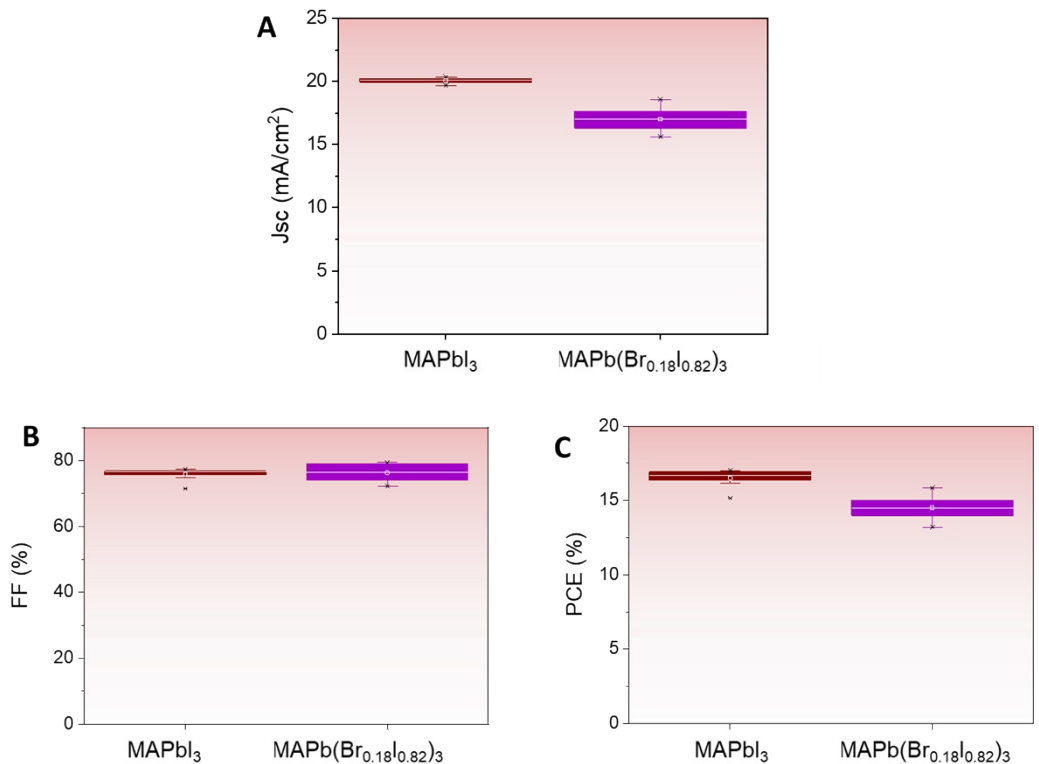


Fig. S11. Photovoltaic parameters of n-i-p PSCs based on PTAA as HTM (A) J_{sc}, (B) FF, and (C) PCE for MAPbI₃ (brown) and MAPb(Br_{0.18}I_{0.82})₃ (purple).

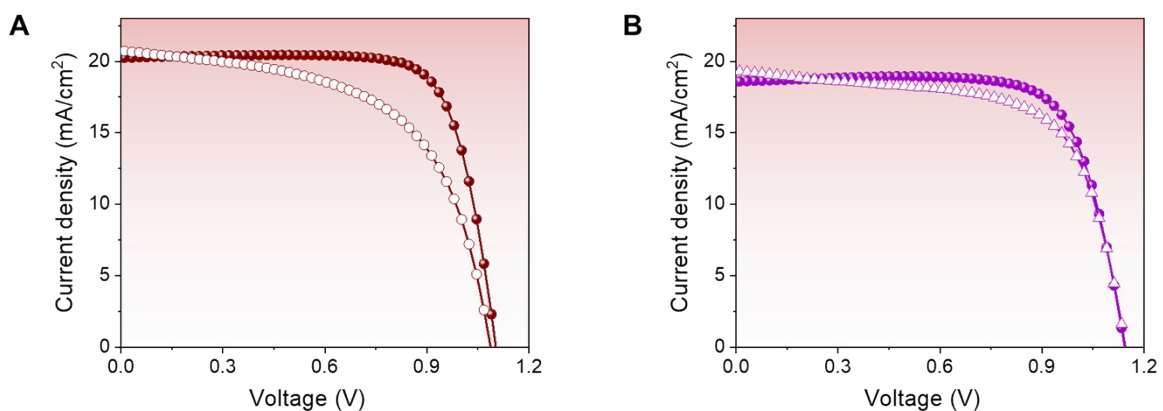


Fig. S12. J-V curves of PTAA HTL based PSCs using (A) MAPbI₃ and (B) MAPb(Br_{0.18}I_{0.82})₃ perovskite compositions taken from reverse (solid) and forward (hollow) scan direction.

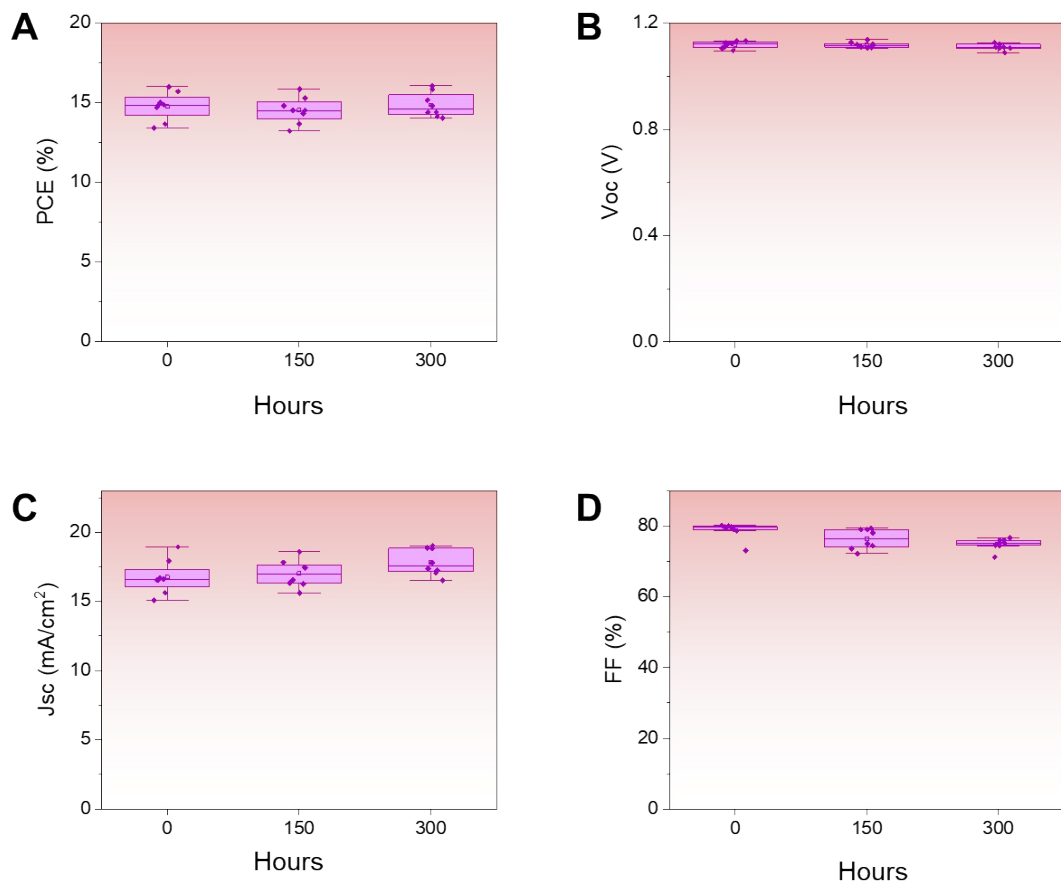


Fig. S13. Shelf stability of $\text{MAPb}(\text{Br}_{0.18}\text{I}_{0.82})_3$ PSCs with PTAA as HTM. Photovoltaic parameters (A) PCE, (B) Voc, (C) Jsc, and (D) FF when stored at room temperature and in a controlled environment with 30% RH for 300 hours.

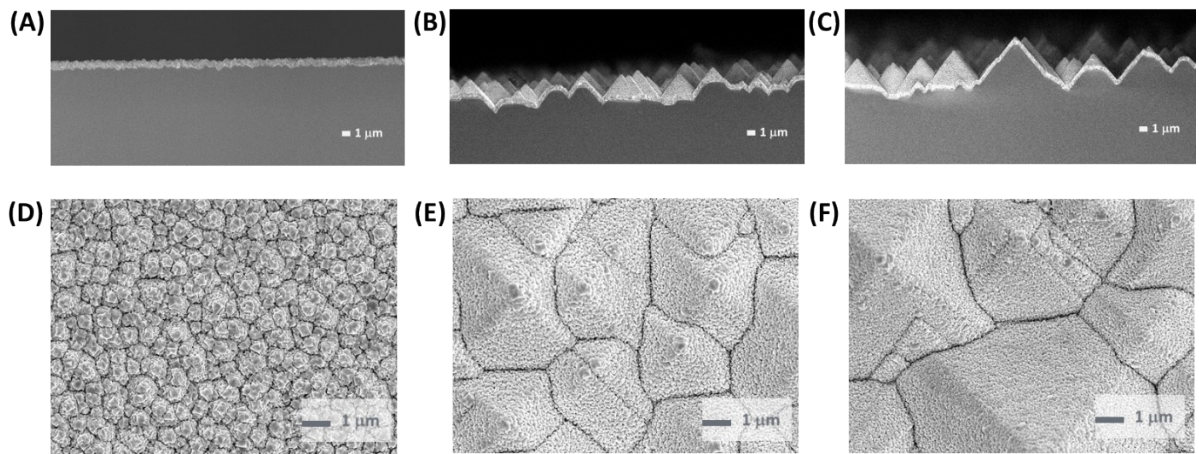


Fig. S14. Cross-section and top view FESEM images of MAPbI₃ deposited on Silicon wafers with three different pyramidal heights (A,D) 1-3 μm , (B,E) 3-5 μm , and (C,F) 5-7 μm of bottom silicon substrates taken at low magnification (scale bar of 1 μm)

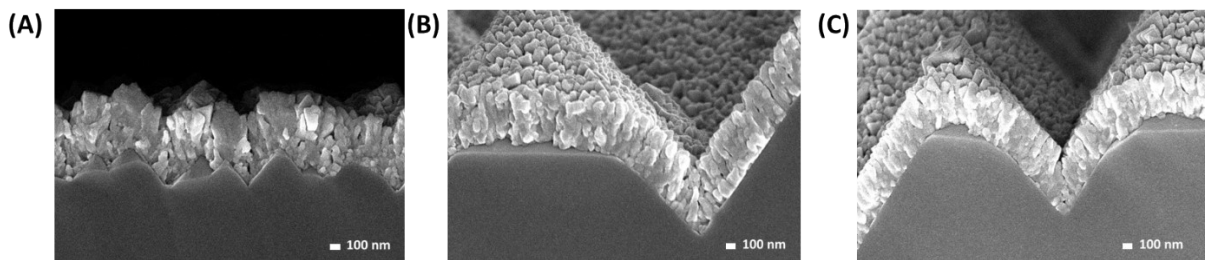


Fig. S15. Cross-section FESEM images of MAPbI₃ deposited on Silicon wafers with three different pyramidal heights (A,D) 1-3 μm , (B,E) 3-5 μm , and (C,F) 5-7 μm of bottom silicon substrates taken at high magnification (scale bar of 100 nm)

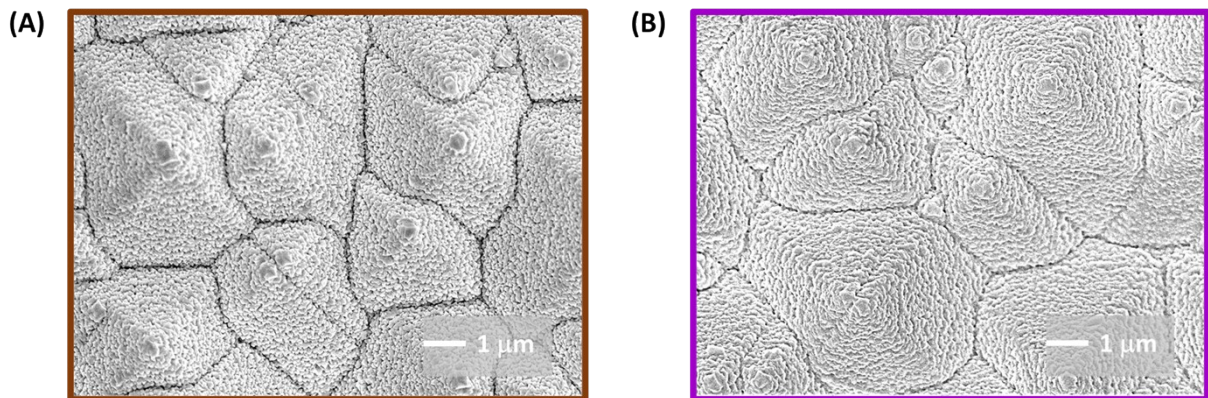


Fig. S16. Top view FESEM of (A) MAPbI₃ (brown) and (B) MAPb(Br_{0.18}I_{0.82})₃ (purple) deposited on a 3-5 μm textured silicon surface taken at low magnification (scale bar of 1 μm)

Table S1. The penetration depth of X-ray into MAPbI_3 film. The penetration depth is calculated according to the formula, $Z = \frac{\sin\alpha}{\mu}$, where α is the incident angle, μ is the attenuation coefficient (1181.5 cm^{-1} for MAPbI_3).

Incident angle (°)	Penetration depth (nm)
2	290±15
5	740±15
8	1200±15

Table S2. Surface binding energies (BE) and the atomic concentrations of both MAPbI_3 and $\text{MAPb}(\text{Br}_{0.18}\text{I}_{0.82})_3$ were measured using XPS.

MAPbI₃

	BE [eV]	Atomic conc. [%]
I 3d	617.70	38.25
C 1s	284.60	46.74
Pb 4f	136.80	14.21
Br 3d	70.30	0.80

MAPb(Br_{0.18}I_{0.82})₃

	BE [eV]	Atomic conc. [%]
I 3d	618.10	32.37
C 1s	284.00	50.16
Pb 4f	137.20	13.52
Br 3d	67.30	3.95

Table S3. Photovoltaic parameters of PSCs based on Spiro-OMeTAD and PTAA HTLs for both MAPbI_3 and $\text{MAPb}(\text{Br}_{0.18}\text{I}_{0.82})_3$ taken from reverse scan directions. The data have been averaged over 20 PSCs in each configuration.

HTL/Perovskite	V _{oc} (V)	J _{sc} (mA/cm ²)	FF (%)	PCE (%)
Spiro/MAPbI ₃	1.05 ± 0.02	20 ± 1	74 ± 3	16 ± 1.0
Spiro/MAPb(Br _{0.18} I _{0.82}) ₃	1.08 ± 0.01	17 ± 1.5	74 ± 2	14 ± 1.5
PTAA/MAPbI ₃	1.08 ± 0.01	20.1 ± 0.2	76 ± 2	16.5 ± 0.6
PTAA/MAPb(Br _{0.18} I _{0.82}) ₃	1.12 ± 0.01	17. ± 1.0	77 ± 3	14.5 ± 0.8